NPS-ME-92-003

NAVAL POSTGRADUATE SCHOOL
Monterey, California

A SURFACE INTEGRAL APPROACH TO THE MOTION PLANNING OF NONHOLONOMIC SYSTEMS

Ranjan Mukherjee

AUGUST 1992

Prepared for:

Mechanical Engineering, Naval Postgraduate School, Monterey CA 93943

NAVAL POSTGRADUATE SCHOOL
Monterey, California

Rear Admiral R.W. West, Jr.
Superintendent

H. Schull
Provost

This report was funded by and prepared for the Department of Mechanical Engineering, Naval Postgraduate School, Monterey, California 93943. Reproduction of all or part of this report is authorized.

This report was prepared by

MATTHEW D. KELLEHER
Chairman
Mechanical Engineering Department

PAUL J. MARTO
Dean of Research

REPORT DOCUMENTATION PAGE

Form Approved
OMB No. 0704-0188

1a. REPORT SECURITY CLASSIFICATION Unclassified	1b. RESTRICTIVE MARKINGS
2a. SECURITY CLASSIFICATION AUTHORITY	3. DISTRIBUTION AVAILABILITY OF REPORT
2b. DECLASSIFICATION/DOWNGRADING SCHEDULE	Approved for public release; distribution unlimited
4. PERFORMING ORGANIZATION REPORT NUMBER(S) NPS-ME-92-003	5. MONITORING ORGANIZATION REPORT NUMBER(S)
6a. NAME OF PERFORMING ORGANIZATION Naval Postgraduate School; 6b OFFICE SYMBOL (If applicable) ME	7a. NAME OF MONITORING ORGANIZATION Naval Postgraduate School
6c. Address (City, State, and ZIP Code) Monterey, CA 93943-5000	7b. ADDRESS (City, State, and ZIP Code) Monterey, CA 93943-5000
8a. NAME OF FUNDING/SPONSORING ORGANIZATION Naval Postgraduate School; 8b OFFICE SYMBOL (If applicable)	9. PROCUREMENT INSTRUMENT IDENTIFICATION NUMBER OM&N Direct Funding
8c. ADDRESS (City, State, and ZIP Code) NPS, Monterey, CA 93943-5000	10. SOURCE OF FUNDING NUMBERS: PROGRAM ELEMENT NO. / PROJECT NO. / TASK NO. / WORK UNIT ACCESSION NO.

11. TITLE (Include Security Classification)
A Surface Integral Approach to the Motion Planning of Nonholonomic Systems

12. PERSONAL AUTHOR(S) MUKHERJEE, RANJAN AND ANDERSON, DAVID P.

13a. TYPE OF REPORT	13b. TIME COVERED	14. DATE OF REPORT (Year, Month, Day)	15. PAGE COUNT
Technical Report	Six months	1992, August, 6	31

16. SUPPLEMENTARY NOTATION The views expressed in this report are those of the authors and do not reflect the official policy or position of the Department of Defense or the U. S. Government.

17. COSATI CODES: FIELD	GROUP	SUB-GROUP

18. SUBJECT TERMS (Continue on reverse if necessary and identify by block number)
Nonholonomic mechanical system, motion planning, configuration space, surface and line integrals, space robot, rolling disk

19. ABSTRACT (Continue on reverse if necessary and identify by block number)

Nonholonomic mechanical systems are governed by constraints of motion that are nonintegrable differential expressions. Unlike holonomic constraints, these differential constraints do not reduce the number of dimensions of the configuration space of a system. Therefore, a nonholonomic system can access a configuration space of dimension higher than the number of degrees of freedom of the system. In this paper, we develop an algorithm for planning admissible trajectories for nonholonomic systems that will take the system from one point in its configuration space to another. In our algorithm we first converge the independent variables to their desired values and then use closed trajectories of the independent variables to converge the dependent variables. We use Stokes's theorem in our algorithm to convert the problem of finding a closed path into that of finding a surface area in the space of the independent variables, such that the dependent variables converge to their desired values as the independent variables traverse along the boundary of this surface area. The use of Stokes's theorem simplifies the motion planning problem and also imparts global characterestics. The salient features of our algorithm are apparent in the two examples that we discuss - a planar space robot and a disk rolling without slipping on a flat surface.

20. DISTRIBUTION/AVAILABILITY OF ABSTRACT	21. ABSTRACT SECURITY CLASSIFICATION
☐ UNCLASSIFIED/UNLIMITED ☐ SAME AS RPT. ☐ DTIC USERS	Unclassified

22a. NAME OF RESPONSIBLE INDIVIDUAL	22b TELEPHONE (Include Area code)	22c. OFFICE SYMBOL
Ranjan Mukherjee	(408) 646-2632	ME/Mk

DD Form 1473, JUN 86 Previous editions are obsolete. SECURITY CLASSIFICATION OF THIS PAGE Unclassified

A Surface Integral Approach to the Motion Planning of Nonholonomic Systems

Ranjan Mukherjee† David P. Anderson‡

Mechanical Engineering Department
Naval Postgraduate School
Monterey, CA 93943

Abstract

Nonholonomic mechanical systems are governed by constraints of motion that are nonintegrable differential expressions. Unlike holonomic constraints, these differential constraints do not reduce the number of dimensions of the configuration space of a system. Therefore a nonholonomic system can access a configuration space of dimension higher than the number of the degrees of freedom of the system. In this paper, we develop an algorithm for planning admissible trajectories for nonholonomic systems that will take the system from one point in its configuration space to another. In our algorithm we first converge the independent variables to their desired values and then use closed trajectories of the independent variable to converge the dependent variables. We use Stokes's theorem in our algorithm to convert the problem of finding a closed path into that of finding a surface area in the space of the independent variables, such that the dependent variables converge to their desired values as the independent variables traverse along the boundary of this surface area. The use of Stokes's theorem simplifies the motion planning problem and also imparts global characteristics. The salient features of our algorithm are apparent in the two examples we discuss - a planar space robot and a disk rolling without slipping on a flat surface.

---

† Assistant Professor
‡ Graduate Student

1. Introduction

Nonholonomic mechanical systems are governed by constraints of motion that are nonintegrable differential expressions of the form

$$\sum_{i=1}^{n} a_{ji}\, dq_i + a_{jt}\, dt = 0, \qquad j = 1, 2, \cdots m \tag{1}$$

where, the q's represent the generalized coordinates, t represents time, and the a's are, in general functions of the q's and t. As a result of the nonintegrable nature of these differential constraints, it is not possible to obtain functions of the form

$$\phi_j(q_1, q_2, \cdots, q_n, t) = 0, \qquad j = 1, 2, \cdots m \tag{2}$$

that will enable us to eliminate some of the dependent variables. Naturally, nonholonomic systems require more coordinates for their description than there are degrees of freedom in the system.

An interesting feature of nonholonomic mechanical systems is their ability to access a configuration space of dimension higher than the number of it's degrees of freedom. A simple example is that of a disk rolling without slipping on a flat surface. The configuration space of the disk rolling on the x-y plane, shown in Fig.1, is described by the four coordinates (x, y, θ, α), but the degrees of freedom of the system is only two because of the following two nonholonomic constraints

$$\begin{aligned} dx - r \sin\alpha\, d\theta &= 0 \\ dy - r \cos\alpha\, d\theta &= 0 \end{aligned} \tag{3}$$

Inspite of having only two degrees of freedom, it is quite intuitive that the rolling disk can arrive at any configuration (x, y, θ, α) from any other, through proper path planning. Such a property is common to nonholonomic mechanical systems and can be attributed to the nonintegrable nature of their differential constraints.

For the rolling disk, our intuition can be strengthened if we consider the following example. Suppose, it is desired that the disk in Fig.1 change its coordinates from (x, y, θ, α) to $(x_d, y_d, \theta, \alpha)$. Then a feasible trajectory would be the path segments AO and OC. The disk would roll forward from A to O, and then roll backward from O to C. The individual path segments AO and OC should have equal lengths such that θ comes back to its initial value at the end of the path. Furthermore, the straight lines AB and CD should be tangent to the path segments AO and OC respectively, at the points A and C. This will ensure that the net change of the variable α will also be zero over the complete path. Such a path can always be planned and this leads us to believe that the dependent variables x and y can indeed be changed arbitrarily through cyclic motion of the independent variables θ and α.

Therefore to converge all the configuration variables of the disk from one set of values to another, we could first converge the independent variables from their initial values to their desired values without being concerned about the evolution of the dependent variables, and then use cyclic motion of the independent variables to converge the dependent variables to their desired values.

In this paper we will develop an algorithm for nonholonomic motion planning - one that will enable us to converge all the configuration variables of a nonholonomic system from one set of values to another. This algorithm will follow a two step procedure - first converge the independent variables, and then use cyclic motion of the independent variables to converge the dependent variables.

The nonholonomic motion planning problem has been the focus of attention of various researchers in the recent past. Specifically, researchers have looked into the problems of mobile robot navigation [1], [5], [6], [10], parking a front-wheel drive car or a car with multiple trailers [9], [10], dextrous manipulation with robotic fingers [2], attitude control of a satellite using two rotors instead of gas-jets, reconfiguration of a space manipulator or a space structure using only internal motion [12], etc. The multibody car system was studied in [10] and it was concluded that it is a well controllable system. This result was obtained by first constructing the control Lie algebra. The controllability was concluded by showing that the rank of the control Lie algebra is equal to the dimension of the state space, at every point in the state space. Such an analysis only provides sufficient conditions for the controllability and is useful for simple nonholonomic systems. It cannot be used to verify the controllability of a complex system like a 6-DOF space robot. Assuming the existence of a feasible trajectory connecting an initial and some desired values of the generalized coordinates, the nonholonomic motion planning of space robots was discussed in [12]. The nonholonomy of a space robot is attributed to the conservation of its angular momentum. A space robot consisting of a six joint manipulator mounted on a space vehicle was described by nine generalized coordinates consisting of six joint angles of the manipulator and the three Euler angles of orientation of the space vehicle. By directly controlling only the joints of the manipulator, it was shown that it is possible to converge all the nine state variables to their desired values. The trajectory was planned using a Lyapunov function and by adopting a bi-directional approach.

An algorithm for steering a general class of nonholonomic systems was developed in [11] using sinusoids. This algorithm was applied for the motion planning of a front wheel drive cart, and reconfiguration of a hopping robot in flight phase. In this algorithm, the independent variables were first steered to their desired configuration ignoring the evolution of the dependent variables. Consequently, the dependent variables were converged to their desired values using closed trajectories of the independent variables. Such an approach was proposed earlier [15], for the motion planning of a space manipulator, where the cyclic motion of the joints of the space manipulator was used to change the orientation of the whole system.

In this paper, we will discuss the motion planning of nonholonomic systems using an algorithm in which the prerogative is to find a closed trajectory of the independent variables that converge the dependent variables to their desired values. In our approach, we use Stokes's theorem to reduce this problem into finding a surface area such that the dependent variables converge to their desired values while the independent variables travel along the boundary of this surface area. The main advantage is the global nature of our planning algorithm, unlike the local path planning approach based on Lyapunov functions [12]. Due to the global nature of the algorithm, questions pertaining to the reachability of the system can be readily answered, problems related to singularity can be tackled, and feasible trajectories can be easily planned even in the presence of additional constraints. For a nonholonomic system like a space robot, these additional constraints may appear in the form of joint limits or obstacles in the workspace. Our algorithm additionally provides us with insight into trajectories that produce repeatable motion. Repeatability in the motion may be simply a desirable property as in the case of space robots, or may even be used for singularity avoidance as in the case of a rolling disk.

This paper is organized as follows. In section 2 we discuss the mathematical preliminaries and the properties of nonholonomic systems. In section 3, we discuss some of the issues related to the motion planning of nonholonomic systems. In section 4, we present our algorithm for the nonholonomic motion planning through examples. Specifically, we discuss the motion planning of a planar space robot and a disk rolling without slipping on a flat surface. The different salient features of our algorithm are apparent in these two examples.

2. Mathematical preliminaries

2.1 Line and surface integrals: Stokes's theorem

In this section we recall Stokes's [8] theorem used for the tranformation of line integrals into surface integrals, and vice verca. The material discussed in this section will serve as a mathematical tool for the trajectory planning of nonholonomic systems.

Theorem 1: Stokes's Theorem Let S be a piecewise smooth oriented surface* in space and let the boundary of S be a piecewise smooth closed curve C. Let $\boldsymbol{v}(x, y, z)$ be a continuous vector function which has continuous first partial derivatives in a domain in space which contains S. Then

$$\int\int_S \boldsymbol{n}^T (\nabla \times \boldsymbol{v})\, dA = \oint_C v_t\, ds \tag{4}$$

where, $\boldsymbol{n}$ is the unit vector normal to the surface S on that side of S which is taken as the positive side. The positive direction along C is then defined as the direction along which

* If a surface S has a unique normal whose direction depends continuously on the points of S, then S is called a smooth surface. If S is not smooth but can be subdivided into finitely many smooth portions, then it is called a piecewise smooth surface.

an observer, traveling on the positive side of S, would proceed in keeping the enclosed area to his left. (see Fig.2 (a)). v_t is the component of $\boldsymbol{v}$ in the direction of the tangent vector of C.

If the direction cosines of the unit vector $\boldsymbol{n}$ normal to the surface S are α, β, and γ, and if $\boldsymbol{v} = v_1\boldsymbol{i} + v_2\boldsymbol{j} + v_3\boldsymbol{k}$, then Stokes's theorem can be written as

$$\int\int_S \left[\left(\frac{\partial v_3}{\partial y} - \frac{\partial v_2}{\partial z}\right)\cos\alpha + \left(\frac{\partial v_1}{\partial z} - \frac{\partial v_3}{\partial x}\right)\cos\beta + \left(\frac{\partial v_2}{\partial x} - \frac{\partial v_1}{\partial y}\right)\cos\gamma\right] dA = \oint_C (v_1\,dx + v_2\,dy + v_3\,dz) \tag{5}$$

If we restrict ourselves to the x-y plane, then Stokes's theorem simplifies to the form

$$\int\int_S \left(\frac{\partial v_2}{\partial x} - \frac{\partial v_1}{\partial y}\right) dx\,dy = \oint_C (v_1\,dx + v_2\,dy) \tag{6}$$

which is essentially a statement of Green's theorem [8]. For the above equation the positive direction of travel along the closed curve C is shown in Fig.2 (b). This directly followed from Eq.(5) where we substituted $(\alpha, \beta, \gamma) = (\pi/2, \pi/2, 0)$. We may change the direction of the closed curve C in Eq.(6) by using $(\alpha, \beta, \gamma) = (\pi/2, \pi/2, \pi)$ in Eq.(5). This will lead to a change in sign of the surface integral in Eq.(6).

Another important theorem that will serve as an important tool for our analysis deals with the path independence of line integrals. This theorem is formally stated next [8]

Theorem 2: Let $\boldsymbol{v} = v_1\,\boldsymbol{i} + v_2\,\boldsymbol{j} + v_3\,\boldsymbol{k}$, and let v_1, v_2, and v_3 be continuous functions of x, y, and z in a domain D of space. Then the line integral

$$\int_C (v_1\,dx + v_2\,dy + v_3\,dz) \tag{7}$$

is independent of path if and only if the differential form under the integral sign in exact in D, or equivalently the integral is zero for every simple closed path in D, or equivalently $\nabla \times \boldsymbol{v} = 0$, everywhere in D.

From the above theorem we see that the necessary and sufficient condition for the exactness of the differential form under the integral sign in Eq.(7) is

$$\frac{\partial v_2}{\partial z} = \frac{\partial v_3}{\partial y}, \qquad \frac{\partial v_3}{\partial x} = \frac{\partial v_1}{\partial z}, \qquad \frac{\partial v_1}{\partial y} = \frac{\partial v_2}{\partial x} \tag{8}$$

2.2 Properties of nonholonomic systems

In this section we discuss some of the important properties of nonholonomic systems. These properties will aid us to develop the motion planning schemes in the section 4.

In section 1 we mentioned that nonholonomic constraints are nonintegrable expressions of the form as in Eq.(1) that cannot be simplified into expressions of the form as in Eq.(2). To further our discussion, we consider again the example of the disk rolling without slipping on a flat surface whose first constraint equation is

$$dx - r \sin\alpha \, d\theta = 0 \tag{9}$$

The above constraint is not an exact differential since there exists no function $\phi(x, \alpha, \theta)$ such that Eq.(9) can be reduced to the form

$$d\phi = \frac{\partial \phi}{\partial x} dx + \frac{\partial \phi}{\partial \alpha} d\alpha + \frac{\partial \phi}{\partial \theta} d\theta = 0$$

Furthermore, Eq.(9) cannot be multiplied by an integrating factor to yield an exact differential. Hence it is not integrable*. It can be shown that the necessary and sufficient condition for the integrability of the differential equation

$$v_1 \, dx + v_2 \, dy + v_3 \, dz = 0$$

is that

$$v_1 \left(\frac{\partial v_2}{\partial z} - \frac{\partial v_3}{\partial y} \right) + v_2 \left(\frac{\partial v_3}{\partial x} - \frac{\partial v_1}{\partial z} \right) + v_3 \left(\frac{\partial v_1}{\partial y} - \frac{\partial v_2}{\partial x} \right) = 0 \tag{10}$$

Applying this criterion to Eq.(9) we confirm that the expression is not integrable. In the more general case, the necessary and sufficient condition that the differential constraint in n variables (Ince, 1956)

$$v_1 \, dx_1 + v_2 \, dx_2 + \cdots + v_n \, dx_n = 0$$

is integrable, is that the set of equations

$$v_\nu \left(\frac{\partial v_\mu}{\partial x_\lambda} - \frac{\partial v_\lambda}{\partial x_\mu} \right) + v_\mu \left(\frac{\partial v_\lambda}{\partial x_\nu} - \frac{\partial v_\nu}{\partial x_\lambda} \right) + v_\lambda \left(\frac{\partial v_\nu}{\partial x_\mu} - \frac{\partial v_\mu}{\partial x_\nu} \right) = 0$$
$$(\lambda, \mu, \nu = 1, 2, \cdots, n) \tag{11}$$

are satisfied simultaneously, and identically.

The nonholonomic property of a dynamical system can also be ascertained from the noninvolutive property of the distribution that spans the tangent space of the system, using Frobenius's theorem. If $\boldsymbol{X}_i \in R^n$, $i = 1, 2, \cdots, m$ denote the vector fields of the system, then the distribution $\boldsymbol{\Delta} = span\{\boldsymbol{X}_1, \boldsymbol{X}_2, \cdots, \boldsymbol{X}_m\}$ is involutive if and only if $\boldsymbol{\Delta}$ is closed under Lie bracket operations. Otherwise, the system is noninvolutive or nonholonomic. In the case of the rolling disk,

$$\dot{\boldsymbol{x}} \triangleq \begin{pmatrix} \dot{x} \\ \dot{y} \\ \dot{\theta} \\ \dot{\alpha} \end{pmatrix} = \boldsymbol{X}_1 \, \dot{\alpha} + \boldsymbol{X}_2 \, \dot{\theta}, \qquad \boldsymbol{X}_1 \triangleq \begin{pmatrix} 0 \\ 0 \\ 0 \\ 1 \end{pmatrix}, \boldsymbol{X}_2 \triangleq \begin{pmatrix} r \sin\alpha \\ r \cos\alpha \\ 1 \\ 0 \end{pmatrix} \tag{12}$$

$$[\boldsymbol{X}_1, \boldsymbol{X}_2] \triangleq \left(\frac{\partial \boldsymbol{X}_2}{\partial \boldsymbol{x}} \right) \boldsymbol{X}_1 - \left(\frac{\partial \boldsymbol{X}_1}{\partial \boldsymbol{x}} \right) \boldsymbol{X}_2 = (r \cos\alpha \quad -r \sin\alpha \quad 0 \quad 0)^T$$

* A differential expression is integrable if it is an exact differential or can be converted into an exact differential after multiplying with an integrating factor.

Clearly, $\boldsymbol{X}_1$, $\boldsymbol{X}_2$, and their Lie bracket $[\boldsymbol{X}_1, \boldsymbol{X}_2]$ are linearly independent. This reconfirms that the rolling disk is a noninvolutive or a nonholonomic system.

The discussion in this section so far enables us to ascertain the nonholonomy of a dynamical system from its differential constraints. We now investigate the manifestation of these nonholonomic constraints.

If a dynamical system is described by n generalized coordinates, and m holonomic constraints of the form as in Eq.(2), the motion of the system is always confined to a manifold or surface of dimension $(n - m)$, which is equal to the number of degrees of freedom of the system. Then, if we specify the $(n - m)$ independent variables, it is possible to uniquely determine the remaining m dependent variables. This is not true when the constraints are nonholonomic or nonintegrable expressions of the form as in Eq.(1). The kinematic effect of a nonholonomic constraint is to constrain the direction of the allowable motions at any given point in the configuration space. But this does not reduce the number of dimensions in the configuration space, nor does it limit the variety of configurations available to the system. As a direct consequence, given the values of the independent variables, it is not possible to uniquely specify the values of the dependent variables of a nonholonomic system. When the independent variables take one set of values from another, the change in the dependent variables depend upon the path taken by the independent variables. Quite naturally, if the independent variables travel along a closed path, the values of the dependent variables at the beginning and end of the path are usually not the same.

The above mentioned property of a nonholonomic system is better understood by the use of Theorem 2 on line integrals. Comparing Eq.(8) (conditions for exactness) to Eq.(10) (conditions for integrability), or directly from the definition of integrability, we know that exactness implies integrability*. Therefore it follows that a nonintegrable expression is not exact. Consider now a nonholonomic system where one of the dependent variables is p and it is constrained by the differential expression $dp = v_1\,dx + v_2\,dy + v_3\,dz$, where x, y, and z are the independent variables. v_1, v_2, and v_3 are continuous functions of x, y, and z. Since the system is nonholonomic or nonintegrable, the differential form $v_1\,dx + v_2\,dy + v_3\,dz$ is not exact. Therefore it follows from Theorem 2 that the change of p is path dependent, and this change is not zero for every closed path. This suggests the following.

1. It is possible to change the coordinates of the dependent variable p of the nonholonomic system using appropriate closed trajectories of the independent variables, and
2. There may exist some closed paths for which the path dependent integral in Eq.(7) will be zero for the nonholonomic system.

On the basis of statement 1 discussed above, we now assume that there exists some closed

* Integrability however does not imply exactness because an integrable differential expression could have become exact only after it was multiplied by some multiplicating factor.

trajectory C of the independent variables x, y, and z that produce a change in the dependent variable p by some desired amount Δp. If (x_0, y_0, z_0) be any point on this closed trajectory and if the initial configuration of the system is (x_0, y_0, z_0, p_0), then after the system moves along C once, its configuration will be $(x_0, y_0, z_0, p_0 + \Delta p)$ (refer to Fig.3 (a)). If the closed curve C was traversed in the opposite direction, then the final configuration of the system would have been $(x_0, y_0, z_0, p_0 - \Delta p)$. Now consider the initial configuration of the system to be (x', y', z', p_0), such that (x', y', z') does not lie on C. Let P be any path segment connecting the point (x', y', z') and any point (x_0, y_0, z_0) on the closed curve C. Let δp denote the change in the dependent variable p, as x, y, and z move along the path segment P from (x', y', z') to (x_0, y_0, z_0). Then, if the system moves from the initial configuration (x', y', z', p_0) to the closed curve C along P, then moves once along the closed curve C, and finally retraces the path P backwards, the configuration of the system at the end of the path (see Fig.3 (b)) will be $(x', y', z', p_0 + \Delta p)$. This is true because the surface integral of the closed curve beginning and ending at the point (x', y', z') is equal to the surface integral of the closed curve C. From this discussion it follows that the closed curve C that can bring about the desired change in the dependent variable can lie anywhere in the space defined by the independent generalized coordinates - it does not have to pass through the initial configuration of the system. Of course, it would be simpler to plan a closed path passing through the initial configuration of the system but then such a path may not be feasible due to singularity problems. We will discuss the singularity problem in the particular situation of a rolling disk, in section 4.

In regards to statement 2 discussed above, we would just like to mention that closed trajectories of the independent variables that result in closed trajectories of the dependent variables (repeatable motion) will be of importance to us in the context of nonholonomic motion planning. Repeatability in the motion may be simply a desirable property as in the case of space robots, or may even be used for singularity avoidance as in the case of a rolling disk. In section 4 we will investigate into the repeatability of the motion of a space robot and of a rolling disk.

3. Issues related to Nonholonomic Motion Planning

The configuration space of a nonholonomic system is described by the set of its independent and the dependent variables. The task of nonholonomic motion planning is to generate trajectories of the independent variables that will take the system from its current configuration to some desired configuration. In the context of the rolling disk, the motion planning would therefore refer to the generation of the θ and α trajectories that will take the system from some initial configuration $(x_i, y_i, \theta_i, \alpha_i)$ to some final configuration $(x_f, y_f, \theta_f, \alpha_f)$.

The question that naturally arises in the context of motion planning is related to the reachability* of the system. In the case of the rolling disk, we know that any configuration of the system is reachable from any other. This follows from our discussion in section 1. For

* A number of researchers like [10], prefer to use the term controllability to reachability,

a multibody car system (a car with n trailers), a mathematical proof of the controllability (reachability) was provided in [1]. For nonholonomic systems in general, the reachability can be ascertained by constructing the control Lie algebra and then using the controllability theorem for nonlinear systems [3]. The control Lie algebra is the smallest involutive distribution containing the span of the vector fields of the system and closed under Lie bracket operations. If the rank of this Lie algebra is full at some configuration C of the system, then there exists a neighborhood N of C whose points represent configurations reachable by the system from C along admissible paths. Clearly, this condition is a local condition. If this condition holds good at every point in the configuration space, then any configuration of the system is reachable from any other using admissible paths.

The controllability (reachability) of a number of simple nonholonomic systems has been verified using the approach discussed above. However, for complicated systems like a 6DOF free-flying space robot [12], this approach is not useful. In the next section we will generate admissible trajectories for simple nonholonomic systems using an algorithm based on Stokes's Theorem. For the two nonholonomic systems that we have considered in section 4, we find that reachability can be easily concluded directly from our algorithm.

An important feature of motion planning algorithms should be their ability to plan admissible trajectories amidst additional constraints. In the case of robot manipulators these additional constraints may appear in the form of obstacles in the workspace or limits imposed on the angular displacement of the joints. In the case of the rolling disk admissible trajectories may have to be planned by avoiding obstacles in the x-y plane. Collision-free trajectories or trajectories amidst additional constraints have been planned using artificial potential functions [7], [13]. In comparison to these approaches, the algorithm discussed in this paper has a global attribute. This feature will be evident in the next section through examples.

While discussing the properties of nonholonomic systems in section 2, we realized that closed trajectories of the independent variables more often result in a change in the dependent variables. This will provide a basis for our motion planning algorithm, where closed trajectories of the independent variables will be suitably planned in order to produce a desired change in the dependent variables. In particular situations we may however be interested in finding closed trajectories of the independent variables that also produce closed trajectories of the dependent variables (repeatable motion). Consider the example of a planar robot in space with two links mounted in a space vehicle, as shown in Fig.4. In this case, the orientation of the space vehicle θ_0 is the dependent variable while the joint variables θ_1 and θ_2 are the independent variables. If this robot is expected to perform a repeatitive task in space, we would expect all the variables θ_0, θ_1, and θ_2 to move along closed trajectories. In the next section, we illustrate repeatability in the case of a two-link space robot, and for a rolling disk. In the case of the rolling disk repeatable motion leads to the generation of singularity free trajectories.

---

and adhere to the terminology used in [14].

4. Nonholonomic motion planning using Stokes's theorem

4.1 Example 1: A planar space robot

In this section we illustrate our algorithm for nonholonomic motion planning using Stokes's theorem, through the example of a 2-DOF planar space manipulator. We consider a planar free-flying space manipulator consisting of two links mounted on a space vehicle, as shown in Fig.4. Such a system can be described by five coordinates: x_0, y_0, and θ_0 representing the position of the center of mass and the orientation of the space vehicle, and θ_1 and θ_2 representing the joint angles of the manipulator. The variables x_0 and y_0 can be eliminated by using the holonomic constraints due to linear momentum conservation. The 2-DOF system is then described by three generalized coordinates θ_i, $i = 0, 1, 2$, and one nonholonomic constraint due to the conservation of angular momentum given by the relation

$$\dot{\theta}_0 = \frac{1}{\Delta}\left(a\,\dot{\theta}_1 + b\,\dot{\theta}_2\right) \tag{13}$$

where,

$$\begin{aligned}
\Delta &\triangleq (\tfrac{1}{2}m_1 + m_2)^2 l_1^2 + \tfrac{1}{4}m_2^2 l_2^2 - (m_0 + \tfrac{1}{2}m_1) m_2 l_1 l_2 \cos\theta_2 - M\left(I + (\tfrac{1}{4}m_1 + m_2) l_1^2 + \tfrac{1}{4}m_2 l_2^2\right) \\
a &\triangleq -\Delta - M\,I_0 \\
b &\triangleq M\left(I_2 + \tfrac{1}{4}m_2 l_2^2 + \tfrac{1}{2}m_2 l_1 l_2 \cos\theta_2\right) - \tfrac{1}{4}m_2^2 l_2^2 - \tfrac{1}{2}m_2(\tfrac{1}{2}m_1 + m_2) l_1 l_2 \cos\theta_2
\end{aligned} \tag{14}$$

and where, m_0, m_1 and m_2 are the masses of the space vehicle and the two links, I_0, I_1 and I_2 are the moments of inertia of the space vehicle and the two links about their center of masses, l_1 and l_2 are the length of the two links, and $M = (m_0 + m_1 + m_2)$ and $I = (I_0 + I_1 + I_2)$.

The configuration of the space manipulator can be described by $(\theta_0, \theta_1, \theta_2)$. Then the path planning problem is to find suitable trajectories for θ_1 and θ_2 that will change the current configuration of the space manipulator to some desired configuration. This immediately raises the question pertaining to the reachability of the system - is it possible to plan trajectories that will take the space manipulator from any initial configuration to any final configuration. The answer to this question is yes, and can be obtained directly from our path planning algorithm, discussed below.

Let the arbitrary initial and desired configurations of the space manipulator be denoted by $(\theta_{0i}, \theta_{1i}, \theta_{2i})$ and $(\theta_{0f}, \theta_{1f}, \theta_{2f})$ respectively. We first converge the joint variables θ_{1i} and θ_{2i} (the independent variables) to their desired values θ_{1f} and θ_{2f} respectively. In this process, let the orientation of the space vehicle (the dependent variable) drift from θ_{0i} to some value θ_{0d}. The task is now to plan a cyclic motion for the joints of the manipulator such that the orientation of the space vehicle changes from θ_{0d} to θ_{0f} while the joint angles come back to

their desired configuration. The associated reachability problem can be solved if we can show that it is possible to change the orientation θ_0 by an arbitrary amount using cyclic motion of the joints, at any joint configuration θ_1 and θ_2. For cyclic motion of the joints, the change in θ_0 is represented as

$$\int d\theta_0 = \oint_C \frac{1}{\Delta}\left(a\, d\theta_1 + b\, d\theta_2\right) \tag{15}$$

where, Δ, a, and b have been defined by Eq.(14), and C in Eq.(15) is a closed curve in the θ_1-θ_2 plane that we will suitably choose. Using Green's theorem given by Eq.(6), the above equation is simplified to

$$\begin{aligned}\int d\theta_0 &= \int\int_S \left[\frac{\partial}{\partial\theta_1}\left(\frac{b}{\Delta}\right) - \frac{\partial}{\partial\theta_2}\left(\frac{a}{\Delta}\right)\right] d\theta_1 d\theta_2 \\ &= M\, I_0 \int\int_S \frac{\partial}{\partial\theta_2}\left(\frac{1}{A + B\cos\theta_2}\right) d\theta_1 d\theta_2\end{aligned} \tag{16}$$

$$\begin{aligned}A &\triangleq \left(\frac{1}{2}m_1 + m_2\right)^2 l_1^2 + \frac{1}{4}m_2^2 l_2^2 - M\left(I + \left(\frac{1}{4}m_1 + m_2\right)l_1^2 + \frac{1}{4}m_2 l_2^2\right) \\ B &\triangleq -\left(m_0 + \frac{1}{2}m_1\right)m_2 l_1 l_2\end{aligned} \tag{17}$$

where, the expressions for a and b were substituted from Eq.(14), and S is the surface in the θ_1-θ_2 plane confined within the closed curve C. Let the desired change in θ_0 be denoted as $\bar{\theta}_0$. Then the path planning problem reduces to the proper selection of the area S in the θ_1-θ_2 plane such that the following equality is satisfied

$$\int\int_S \frac{\partial}{\partial\theta_2}\left(\frac{1}{A + B\cos\theta_2}\right) d\theta_1 d\theta_2 = \frac{\bar{\theta}_0}{M\, I_0} \triangleq k \tag{18}$$

If we choose a rectangular path in the θ_1-θ_2 plane, such that the sides of this rectangle are parallel to the θ_1 and θ_2 axes, then the above identity reduces to

$$(\theta_{1u} - \theta_{1l})\left[\frac{1}{A + B\cos\theta_{2u}} - \frac{1}{A + B\cos\theta_{2l}}\right] = k \tag{19}$$

where, θ_{1l} and θ_{1u} denote the lower and upper extremities of θ_1 in the rectangular path while θ_{2l} and θ_{2u} denote the same for θ_2.

The reachability of the system can be proven by showing that there exists a surface S such that the equality in Eq.(18) can be satisfied for any arbitrary value of k. The initial values of θ_1 and θ_2 does not necessarily have to lie on the boundary of this surface S. This follows from our discussion in section 2.2. We first note that if the identity in Eq.(18) can be satisfied for some value of k by traveling along the boundary of the area S in the positive direction, then the same identity can be satisfied for $-k$ by simply traveling along the boundary in the negative direction. Furthermore, if the identity can be satisfied for some value of k by traveling once along the boundary of S, then the identity can be

satisfied for the value nk, $n = 1, 2, \cdots$, by traveling n times along the boundary in the same direction. Clearly, the reachability problem reduces to showing that the identity in Eq.(18) can be satisfied for any value of $k \in [0, \epsilon)$, where ϵ is some positive small number. For a rectangular area S, this is easy to prove. We can always choose the values of θ_{2l} and θ_{2u} in Eq.(19) such that the quantity α defined as

$$\alpha = \left(\frac{1}{A + B\cos\theta_{2u}} - \frac{1}{A + B\cos\theta_{2l}} \right)$$

is not equal to zero. Then it is quite obvious that $(\theta_{1u} - \theta_{1l})$ can be chosen to be equal to k/α such that the identity in Eq.(19) can be satisfied for any value of $k \in [0, \epsilon)$.

We now illustrate our path planning algorithm with the help of a simple example. We consider a space manipulator (refer to Fig.4) of material alluminum, whose kinematic and dynamic parameters are given below in SI units:

Kinematic and Dynamic parameters

	Mass	Inertia	Length
Vehicle	27.440	1.520	
Link-1	5.380	0.115	$l_1 = 0.50$
Link-2	2.640	0.028	$l_1 = 0.35$

Let the initial configuration of the system be $(\theta_{0i}, \theta_{1i}, \theta_{2i}) \equiv (0.0, 15.0, 15.0)$ degrees, and the final configuration be $(\theta_{0f}, \theta_{1f}, \theta_{2f}) \equiv (-20.0, 45.0, 0.0)$ degrees. We first converge θ_1 and θ_2 from their current values to their desired values using the straight line trajectory OA, as shown in Figs.5 and 6. In this process, the orientation of the space vehicle drifts from 0.0 degrees to $\theta_{0d} = -12.87$ degrees, as shown in Fig.6. Therefore, $\bar{\theta}_0 = (\theta_{0f} - \theta_{0d}) = -7.13$ degrees, or -0.1244 radians. We now plan a cyclic motion of the joints such that after three complete cycles of the joint motion the orientation of the space vehicle changes by the desired amount. Then, for each cycle, the required change of orientation would be $-0.1244/3.0 = -0.0415$ radians. Using this value for $\bar{\theta}_0$, the value of k in Eq.(18) is computed to be -7.696×10^{-4}. With the complete liberty to choose the closed path in the joint space, we choose the simple directed path given by the rectangle $ABCD$ in Fig.5. The closed curve is chosen such that the intermediate configuration of the system - point A, lies on this closed curve. The surface integral in Eq.(18) then simply reduces to

$$\begin{aligned} \int\int_{ABCD} d\left(\frac{1}{A + B\cos\theta_2} \right) d\theta_1 &= (\theta_{1f} - \theta_{1i}) \left(\frac{1}{A + B\cos\theta_{2f}} - \frac{1}{A + B\cos\theta_{2i}} \right) \\ &= (\lambda - \frac{\pi}{4}) \left(\frac{1}{A + B\cos\gamma} - \frac{1}{A + B\cos 0} \right) \end{aligned} \tag{20}$$

where, λ and γ have to be chosen appropriately. We choose $\lambda = 125.0$ degrees *i.e.* 2.181 radians. Then using the values of $A = -89.848$ and $B = -13.92$ from Eq.(17) and the table above, we obtain the value of $\gamma = 0.596$ radians or 53.36 degrees. For this choice of λ and γ, the evolution of all the configuration variables for the path $OABCD$ are shown in Fig.6.

We would like to mention a few points at this juncture. For the same set of values of γ and λ, there are infinite paths that will produce the same change in the orientation θ_0. As for example, the directed paths $OABCDA$ (taken from Fig.5) and $OADMNA$ in Fig.7 will produce the same change in the orientation θ_0. In both these cases the intermediate configuration $(\theta_{0d}, \theta_{1f}, \theta_{2f})$ - point A, lie on the closed curves $ABCD$ and $ADMN$. This only simplifies the motion planning problem but is not a necessary condition, as we have already discussed in section 2.2. Area $ADMN$ can be concieved as a translation of the area $ABCD$ to the left along BA. In fact, the translation of the area $ABCD$ by any amount along the line BA will result in feasible closed trajectories. This follows directly from the expression for the surface integral in Eq.(20). We see that the surface integral in Eq.(20) depends upon the difference of the values of θ_{1f} and θ_{1i}, but not individually on θ_{1f} and θ_{1i}. There are also infinite other combinations of λ and γ values that we can choose to satisfy Eq.(20). And there is even more flexibility when we can suitably choose the number of cycles of joint motion that will produce the desired change in the orientation θ_0. As for example, in the particular situation discussed above, the directed path $AXYZ$ can bring about the same change in θ_0 in four cycles of the joint motion that the paths $ABCD$ and $ADMN$ can bring about in three cycles. The path $AXYZ$ was obtained by choosing $\gamma = 75.0$ degrees which led to the value of $\lambda = 76.084$ degrees.

We next consider the practical situation where the trajectory of the system may have to be planned subject to the joint limits $|\theta_i| \leq 120$ degrees. Then for the above example, the trajectories $ADMN$ and $AXYZ$ in Fig.7 would be feasible whereas the trajectory $ABCD$ would not be feasible. It is quite clear that our path planning algorithm provides us with the flexibility in choosing trajectories that can satisfy additional constraints, like joint limits in the case of space robots.

We complete this section with a discussion on repeatable motions of the space robot. In particular situations, a space robot may be expected to perform a repeatative task in space. In such a situation the end-effector of the robot as well as the configuration variables of the robot will all have to move along closed trajectories. If the joints of the robot, shown in Fig.4, move along closed trajectories, the dependent variables x_0 and y_0 will always move along closed trajectories because of the holonomic nature of the linear momentum constraints. The dependent variable θ_0 will however not move along a closed trajectory in the general case. If the net change in θ_0 were also to be zero as the joints moved along a closed rectangular path, then from Eq.(19), the necessary conditions that would have to be satisfied are $\theta_{1u} = \theta_{1l}$, or $\cos\theta_{2u} = \cos\theta_{2l}$ (assuming a rectangular path in the θ_1-θ_2 plane). The first condition leads us to the trivial case where the first joint of the robot will have to be kept fixed. The second condition tells us that repeatability is assured for $\theta_{2u} + \theta_{2l} = 2n\pi$, $n = 0, \pm1, \pm2, \cdots$. In the previous example that we considered, we found that we had a significant amount of flexibility in choosing the closed trajectories. Though the condition $\theta_{2u} + \theta_{2l} = 2n\pi$, $n = 0, \pm1, \pm2, \cdots$, will restrict our choices, we should still be able to choose from a variety of paths that will produce repeatable motion.

4.2 Example 2: A disk rolling without slipping on a flat surface

We revisit the classical example of the disk rolling without slipping on a flat surface and this time we apply our algorithm for its nonholonomic path planning. The configuration space of the rolling disk, as discussed in section 1, is described by (x, y, θ, α). The independent variables of the system are θ and α, and x and y are the dependent variables constrained by the expressions given in Eq.(3). While planning a path from an initial configuration of the disk $(x_i, y_i, \theta_i, \alpha_i)$ to some desired configuration $(x_f, y_f, \theta_f, \alpha_f)$, we first converge the independent variables to their desired values using some simple trajectory without being much concerned about the evolution of the dependent variables. This trajectory may however be important so as to avoid a singularity problem, which we shall discuss soon. At the end of this trajectory (path segment OP in Fig.8), the dependent variables are assumed to drift to values x_d and y_d. Now the task is to plan a closed path for the independent variables θ and α such that the dependent variables x and y change their values from x_d and y_d to x_f and y_f respectively. Let C be such a closed path in the θ-α plane. Then the change of the variables x and y are represented as

$$(x_f - x_d) = \oint_C r \sin\alpha d\theta = \int\int_S -r \cos\alpha \, d\theta \, d\alpha \tag{21}$$

$$(y_f - y_d) = \oint_C r \cos\alpha d\theta = \int\int_S r \sin\alpha \, d\theta \, d\alpha \tag{22}$$

where, we applied Green's theorem, given by Eq.(6), to convert the line integral into the surface integral. Therefore, S is the surface in the θ-α plane within the closed curve C. We choose the closed curve C as the directed rectangular path $PQRSP$ as shown in Fig.8. For this rectangular path $PQRSP$, Eqs.(21) and (22) yield

$$(x_f - x_d) = -2\,a\,r \sin(b/2)\,\cos(\alpha_f + b/2) \tag{23}$$

$$(y_f - y_d) = 2\,a\,r \sin(b/2)\,\sin(\alpha_f + b/2) \tag{24}$$

Assuming $b \neq 2n\pi$, $n = \pm 1, \pm 2, \cdots$, we solve for a and b as follows

$$b = 2\left[-\alpha_f + \arctan 2\,(y_f - y_d, x_d - x_f)\right], \qquad 0 < b < 4\pi \tag{25}$$

$$a = \frac{\left\{(x_f - x_d)^2 + (y_f - y_d)^2\right\}^{1/2}}{2\,r\,\sin(b/2)}, \qquad a > 0 \tag{26}$$

As the disk would move along the sides QR and SP of the rectangular path $PQRSP$ in Fig.8, the value of α would have to change in the absence of rolling. This may not be simple to achieve in practice, as for example in the case of an unicyclist. We therefore modify our rectangular path to the path $PQMNP$ in Fig.8 where α would change only when the disk is rolling. It is easy to show that surface the integral in Eq.(21), as in Eq.(22), will have the same value when the closed curve C is the rectangle $PQRSP$ or the parallelopiped $PQMNP$.

Equation (26) has a singularity for

$$\arctan 2\,(y_f - y_d, x_d - x_f) = \alpha_f \tag{27}$$

and there are three simple ways to overcome this singularity problem. One way would be to arrive from the initial configuration to a different intermediate configuration *i.e.* at a different set of values x_d and y_d, that would not satisfy Eq.(27). This would require us to choose a different trajectory from O to P (see Fig.8). The second alternative would be to set an intermediate goal x'_f, y'_f and first move to this configuration from x_d, y_d using cyclic motion of the independent variables. Then the remaining task would be to plan a second cyclic motion of the independent variables such that the dependent variables would converge to x_f, y_f from their values x'_f, y'_f. The smart alternative would be to follow the three step procedure explained below and diagrammatically shown in Fig.9.

1 Change the present configuration variables θ_f and α_f to some other values θ'_f and α'_f using any trajectory OR, such that $\alpha'_f \neq \alpha_f$, at R. Ignore the evolution of the variables x and y that take the new values x'_d, y'_d at R from their values x_d, y_d at O.
2 Construct any closed path C passing through R, that will change the x and y variables by amounts $(x_f - x_d)$ and $(y_f - y_d)$ respectively. If we choose a rectangular path, or the equivalent parallelogram path, then the dimensions of this path would be computed from Eqs.(24) and (25) only by replacing α_f in Eq.(24) by α'_f. Move along this closed trajectory once to come back to R where $\theta = \theta'_f$ and $\alpha = \alpha'_f$.
3 Retrace backwards the trajectory OR to move from R to O. At O the configuration of the system would be $(x_f, y_f, \theta_f, \alpha_f)$.

The above procedure for singularity avoidance follows from our discussion in section 2.2. This procedure is also recommended for avoiding points close to singular points. At points close to the singularity, trajectories tend to become infeasible due to the large magnitude of a, as evident from Eq.(26).

We are now convinced that any configuration of the rolling disk $(x_f, y_f, \theta_f, \alpha_f)$ can be reachable from any initial configuration $(x_i, y_i, \theta_i, \alpha_i)$ by using the motion planning algorithm discussed in this section. Though in certain situations, there may be a singularity problem, this problem can be easily overcome. The singularity that we may encounter is however not a physical singularity, it is rather an algorithmic singularity. The singularity problem can be completely removed by adopting a slightly different algorithm. This algorithm, to be discussed shortly, uses the repeatable motion of one of the dependent variables. This algorithm will further strengthen our conviction on the reachability issue of the rolling disk.

We illustrate our path planning algorithm with the help of a simple example. In this example we come close to the singularity and we tactfully avoid it using the algorithm discussed above. Consider a disk of radius $r = 0.25\,m$ which is at its current configuration $(x_i, y_i, \theta_i, \alpha_i) \equiv (0.0, 0.0, 0.0, 0.0)$ metres, degrees. Suppose the desired configuration of this disk is $(x_f, y_f, \theta_f, \alpha_f) \equiv (-0.4, 1.0, 180.0, 22.5)$ metres, degrees. We first converge the vari-

ables θ and α to their desired values using the simple straight line path OZ, as shown in Fig.10. The coordinates of x and y at the end of this path will be 0.1522 and 0.7654 metres respectively (obtained through numerical simulation). Using Eqs.(25) and (26), we solve for a and b as $b = 0.01808$ and $a = 132.72$ radians respectively. Clearly, we are close to a singular configuration. In the light of the discussion on singularity avoidance, we adopt the following measure. We have the complete liberty to choose θ'_f and α'_f (point R in Fig.9), with the only restriction that $\alpha'_f \neq \alpha_f$. We choose $(\theta'_f, \alpha'_f) = (\theta_i, \alpha_i) = (0.0, 0.0)$. And we change θ_f and α_f to θ_i and α_i by retracing the path OZ backwards (see Fig.10). We therefore come back to the initial configuration where $(x, y, \theta, \alpha) = (x_i, y_i, \theta_i, \alpha_i)$. Now we substitute the value of α_i in place of α_f in Eq.(25) and solve for a and b from Eqs.(25) and (26). We obtain $b = 0.8034$ radians or 46.03 degrees and $a = 3.068$ radians or 175.78 degrees. In Fig.10, the path $OPQRO$ is the closed path constructed with these values of a and b. Due to the motion along this closed path the change in the x and y coordinates will be $(x_f - x_d) = (-0.4 - 0.1522) = -0.5522$ metre and $(y_f - y_d) = (1.0 - 0.7654) = 0.2346$ metre respectively. Therefore the coordinates at O of the dependent variables after the motion along the closed path will be $x = -0.5522$ and $y = 0.2346$ metres. We finally trace the straight line path from O to Z. Due to this motion the change in the x and y coordinates will be $(x_d - x_i) = (0.1522 - 0.0) = 0.1522$ metre and $(y_d - y_i) = (0.7654 - 0.0) = 0.7654$ metre respectively. Therefore, the coordinates at Z will be $(-0.5522 + 0.1522) = -0.4$ metre and $(0.2346 + 0.7654) = 1.0$ metre respectively. The coordinates of the independent variables at Z are obviously $\theta = 180.0$ degrees and $\alpha = 22.5$ degrees. Looking back at the entire motion, we realize that the initial path from O to Z and back to O is redundant. Therefore, the path that will be sufficient for converging all the variables will be $OPQROZ$, as shown in Fig.10. The closed path $OPQRO$ is chosen to be a parallelogram instead of a rectangle for reasons we have already discussed earlier in this section. The complete path $OPQROZ$ is quite different from paths that are generated in the absence of singularity. In the absence of singularity, the complete path consists of an initial path segment followed by a closed loop in the θ-α plane. In the particular example that we have considered, we had a singularity and the complete path consisted of a closed loop path followed by a simple path segment. The simulation results of this particular example have been shown in Fig.11. The points O, P, Q, R, and Z in Fig.11 correspond to the same points in Fig.10.

The singularity problem discussed above arises due to the particular nature of our algorithm where we converge both the dependent variables x and y simultaneously using closed trajectories of the independent variables. We have seen that this is not at all a serious problem. However, this problem can be completely eliminated by adopting a slightly different algorithm. The idea behind this algorithm is to use repeatable motion of one of the dependent variables. This algorithm is discussed next.

In our singularity free algorithm, we will first converge the independent variables θ and α from their initial values (θ_i, α_i) to their desired values (θ_f, α_f). Let us suppose that the dependent variables x and y change their coordinates from x_i and y_i to x_d and y_d respectively. We will next converge x to its desired value x_f using closed trajectories of the

independent variables without being concerned about the evolution of the y coordinate. Specifically, we will use Eq.(23), where we will have the liberty to choose a set of values a and b. Let us suppose that the dependent variable y drift from its previous coordinate y_d to y'_d in this process. We will finally converge y from its present coordinate y'_d to its desired value y_f using closed trajectories of the independent variables that will also produce a closed trajectory of the dependent variable x, *i.e.* a repeatable motion in the x coordinate. From Eqs.(23) and (24) it follows that the correct choice of the variables a and b for this repeatable motion should be

$$b = -2\alpha_f \pm n\pi, \qquad a = \frac{\Delta y}{2r\cos\alpha_f}, \quad \alpha_f \neq \pm(2n+1)\pi/2, \qquad n = 0, 1, 2, \cdots \tag{28}$$

where $\Delta y = (y_f - y'_d)$, and b will be chosen such that $b > 0$. The magnitude of a can however be positive or negative. We will use the absolute value of a to construct the parallelogram path in the θ-α plane. If the sign of a is obtained negative from Eq.(28), then the use of the positive value will bring about a change in the y coordinate by an amount $-\Delta y$ instead of Δy. This problem can be simply solved by changing the direction of travel along the closed path. This idea has been appropriately demonstrated in the next simulation.

As an alternative, we could also converge the dependent variable y before we converge the dependent variable x. In that case, after the initial motion from the configuration $(x_i, y_i, \theta_i, \alpha_i)$ to the configuration $(x_d, y_d, \theta_f, \alpha_f)$, we would suitably choose a and b in Eq.(24) such that y converges from y_d to y_f. At this stage we will not be concerned about the evolution of the x coordinate, which will probably drift from x_d to x'_d. Finally, we will change the variable x by an amount $\Delta x = (x_f - x'_d)$ using closed trajectories of θ and α that will also produce a closed trajectory of y, *i.e.* a repeatable motion in the y coordinate. From Eqs.(23) and (24) it then follows that the correct choice of the variables a and b would be

$$b = 2(n\pi - \alpha_f), \qquad a = \frac{\Delta x}{2r\sin\alpha_f}, \quad \alpha_f \neq \pm n\pi, \qquad n = 0, 1, 2, \cdots \tag{29}$$

where, b will be chosen such that it is a positive number, and the absolute value of a will be used to construct the trajectory. The direction of travel along the closed trajectory should be along the positive or the negative direction depending upon whether the sign of a comes out to be positive or negative in Eq.(29).

From the two alternatives we conclude that if the final value of α is such that $\alpha_f = \pm(2n+1)\pi/2$, for $n = 0, 1, 2, \cdots$, then we will first converge y and then converge x. If $\alpha_f = \pm n\pi$, for $n = 0, 1, 2, \cdots$, then we will first converge x and then converge y. For $\alpha_f \neq n\pi/2$, for $n = 0, 1, 2, \cdots$, either of the two alternatives mentioned above can be adopted.

To illustrate the efficacy of this singularity free algorithm, we consider the same example we have considered before. The initial configuration of the disk of radius $r = 0.25$ metres is $(x_i, y_i, \theta_i, \alpha_i) \equiv (0.0, 0.0, 0.0, 0.0)$ metres, degrees, and its desired configuration is $(x_f, y_f, \theta_f, \alpha_f) \equiv (-0.4, 1.0, 180.0, 22.5)$ metres, degrees. We first converge the independent variables using a straight line path (path segment OP in Figs.12 and 13) in the θ-α

plane. At the end of this path the configuration of the system is found to be $(x, y, \theta, \alpha) = (0.1522, 0.7654, 180.0, 22.5)$ metres and degrees respectively. Since $\alpha_f = 22.5$ degrees $\neq n\pi/2$, for $n = 0, 1, 2, \cdots$, therefore we can choose to first converge x or y. We choose to converge x first. In Eq.(23), we substitute $x_f = -0.4$ metres, $x_d = 0.1522$ metres, and $\alpha_f = 22.5$ degrees. Choosing $b = 60$ degrees or 1.047 radians, we obtain $a = 3.628$ radians or 207.87 degrees. For these values of a and b, the closed path is given by $PQRSP$ in Fig.12. After moving along this path, the y variable drifts from $y_d = 0.7654$ metres to $y'_d = 1.485$ metres, as shown in Fig.13, whereas the x coordinate converges to its desired value. Now the task is to generate a closed path in the θ-α plane that will cause a repeatable motion in x but will converge y to $y_f = 1.0$ metre. Using Eq.(28) we arrive at $b = 135$ degrees, or 2.356 radians and $a = -1.05$ radians, or 60.15 degrees. For these particular values of a and b, the closed trajectory is given by $PXYZP$ in Fig.12. Due to the negative value of a the direction of this closed path is opposite to our usual convention. The entire motion of the system can be obtained by eliminating the redundant path segment SPS. Therefore the complete motion of the system would be $OPQRSXYZP$, as shown in both Figs.12 and 13.

5. Conclusion

A motion planning algorithm for nonholonomic mechanical systems was presented in this paper. In this algorithm, the independent variables of the system were first converged to their desired values. Subsequently, the dependent variables were converged using closed trajectories of the independent variables. The task of motion planning was simplified using Stokes's theorem. This reduced the task of finding closed trajectories of the independent variables into that of finding a surface area in the space of the independent variables such that the dependent variables converged to their desired values while the independent variables traversed along the boundary of this surface area. The motion planning algorithm was found to have certain global attributes due to which questions pertaining to the reachability of the system could be easily answered and the motion could be planned amidst additional constraints. The salient features of the algorithm was aptly illustrated through the examples of a planar space robot and a disk rolling without slipping on a flat surface.

REFERENCES

[1] Barraquand, J., and Latombe, J.C., 1990, "Controllability of mobile robots with kinematic constraints", Technical Report: STAN-CS-90-1317, Stanford University.

[2] Cole, A., Hauser, J., and Sastry, S., 1989, "Kinematics, and control of a multifingered robot hand with rolling contact", IEEE Transactions on Automatic Control, 34(4).

[3] Hermann and Krener, "Nonlinear controllability and observability", IEEE Transactions on Automatic Control, 22(5).

[4] Ince, E.L., 1956, "Ordinary Differential Equations", Dover Publications, New York.

[5] Jacobs, P., and Canny, J., 1990, "Robust motion planning for mobile robots", IEEE

International Conference on Robotics and Automation, Cincinnati.

[6] Jacobs, P., Rege, A., and Laumond, J.P., 1991, "Non-holonomic motion planning for Hilare-like mobile robots", International Symposium on Intelligent Robotics, Bangalore, India.

[7] Khatib, O., 1985, "Real-time obstacle avoidance for manipulators and mobile robots", IEEE International Conference on Robotics and Automation, pp. 500-505.

[8] Kreyzig, E., 1972, "Advanced Engineering Mathematics", Wiley Eastern Limited.

[9] Lafferriere, G., and Sussman, H.J., 1990, "Motion planning for controllable systems without drift", IEEE International Conference on Robotics and Automation: Workshop on Nonholonomic Motion Planning.

[10] Laumond, J.P., 1990," Nonholonomic Motion planning versus Controllability via the Multibody Car system example", Technical Report: STAN-CS-90-1345, Stanford University.

[11] Murray, R.M., and Sastry, S.S., 1991, "Nonholonomic Motion Planning using Sinusoids", 1991 IEEE International Conference on Robotics and Automation: Workshop on Nonholonomic Motion Planning.

[12] Nakamura, Y., and Mukherjee, R., 1991, "Nonholonomic Motion Planning of Space Robots via a Bi-Directional Approach", IEEE Transactions on Robotics and Automation, Vol. 7, No. 4, pp. 500-514.

[13] Mukherjee, R., and Nakamura, Y., 1991, "Nonholonomic Redundancy of Space Robots and its utilization via hierarchical Liapunov functions", American Control Conference, Vol. 2, pp. 1491-1496.

[14] Sussman, H.J., 1982, "Lie brackets, real analyticity and geometric control", Differential Geometric Control Theory, Eds. Brockett, Millman, Sussman, Birkhauser.

[15] Vafa, Z., and Dubowsky, S., 1987, "On the dynamics of manipulators in space using the virtual manipulator approach", IEEE International Conference on Robotics and Automation.

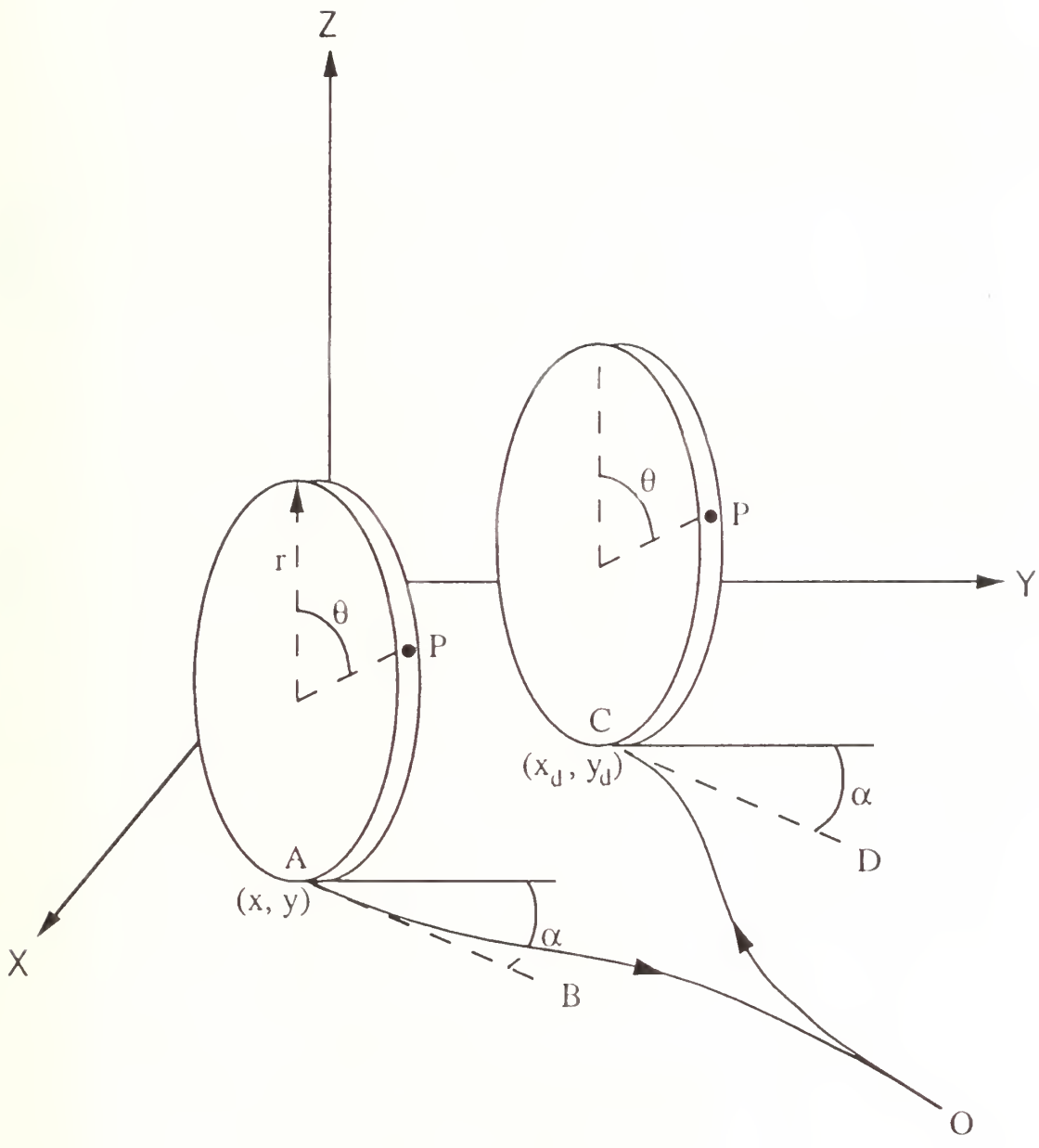

Figure 1. A disk rolling on a flat surface is described by four configuration variables: x, y, θ, α. The disk has however two degrees of freedom due to the presence of two nonholonomic constraints.

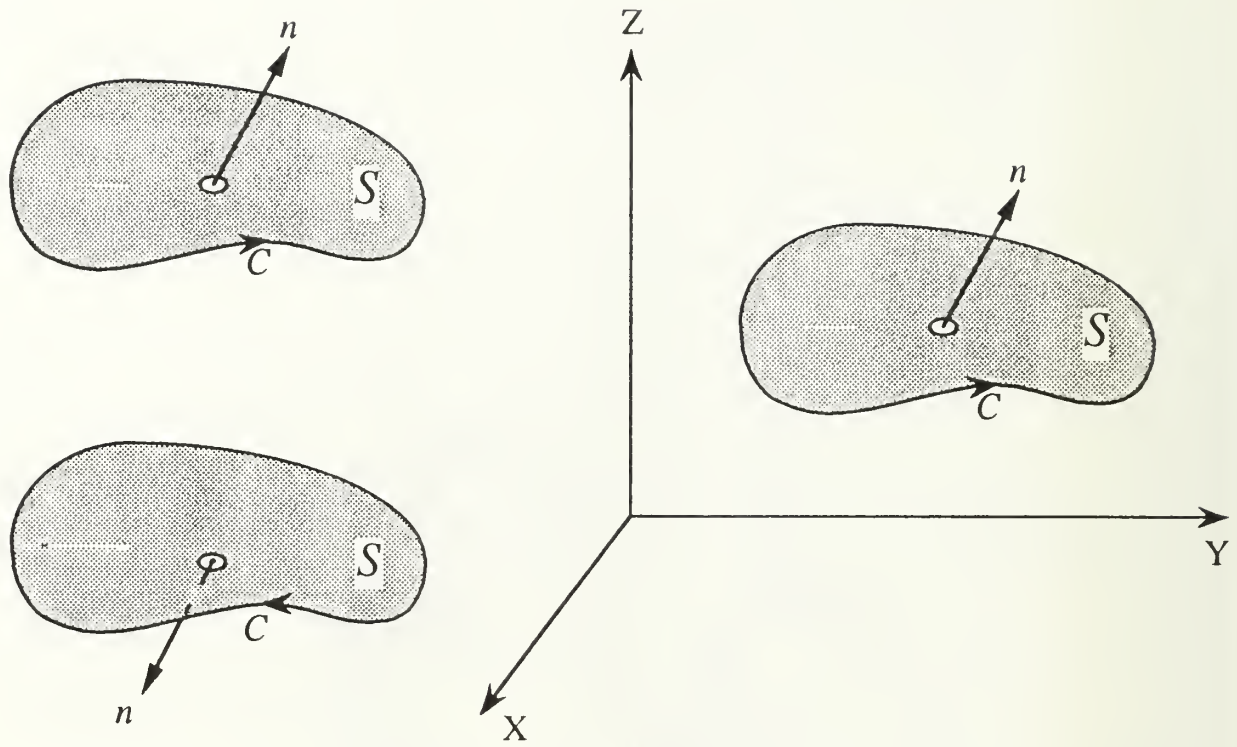

Figure 2 (a). Positive direction of travel along the closed curve C in Stokes Theorem

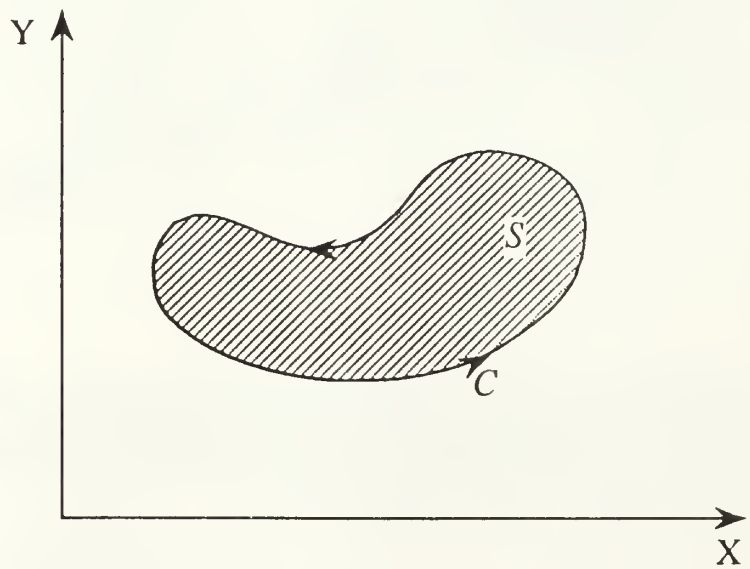

Figure 2 (b). Positive direction of travel along the closed curve *C* in Green's Theorem

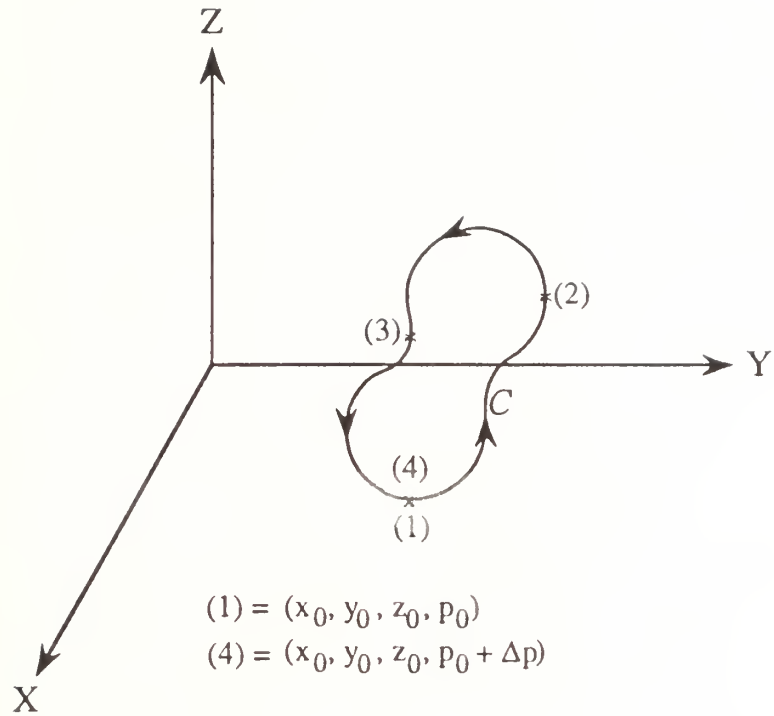

Figure 3 (a). The closed trajectory *C* in the independent variables x, y, and z produces a change in the dependent variable p by an amount Δp. The initial configuration of the system - (1), lies on this closed trajectory.

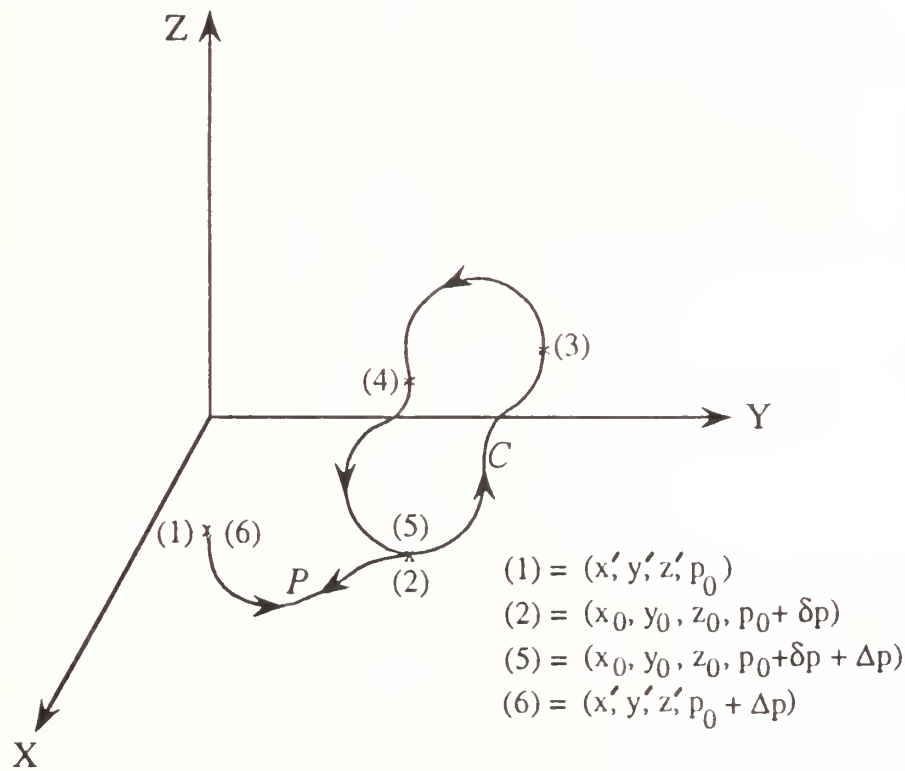

Figure 3 (b). The closed trajectory *C* in the independent variables x, y, and z produces a change in the dependent variable p by an amount Δp. The initial configuration of the system - (1), does not lie on this closed trajectory.

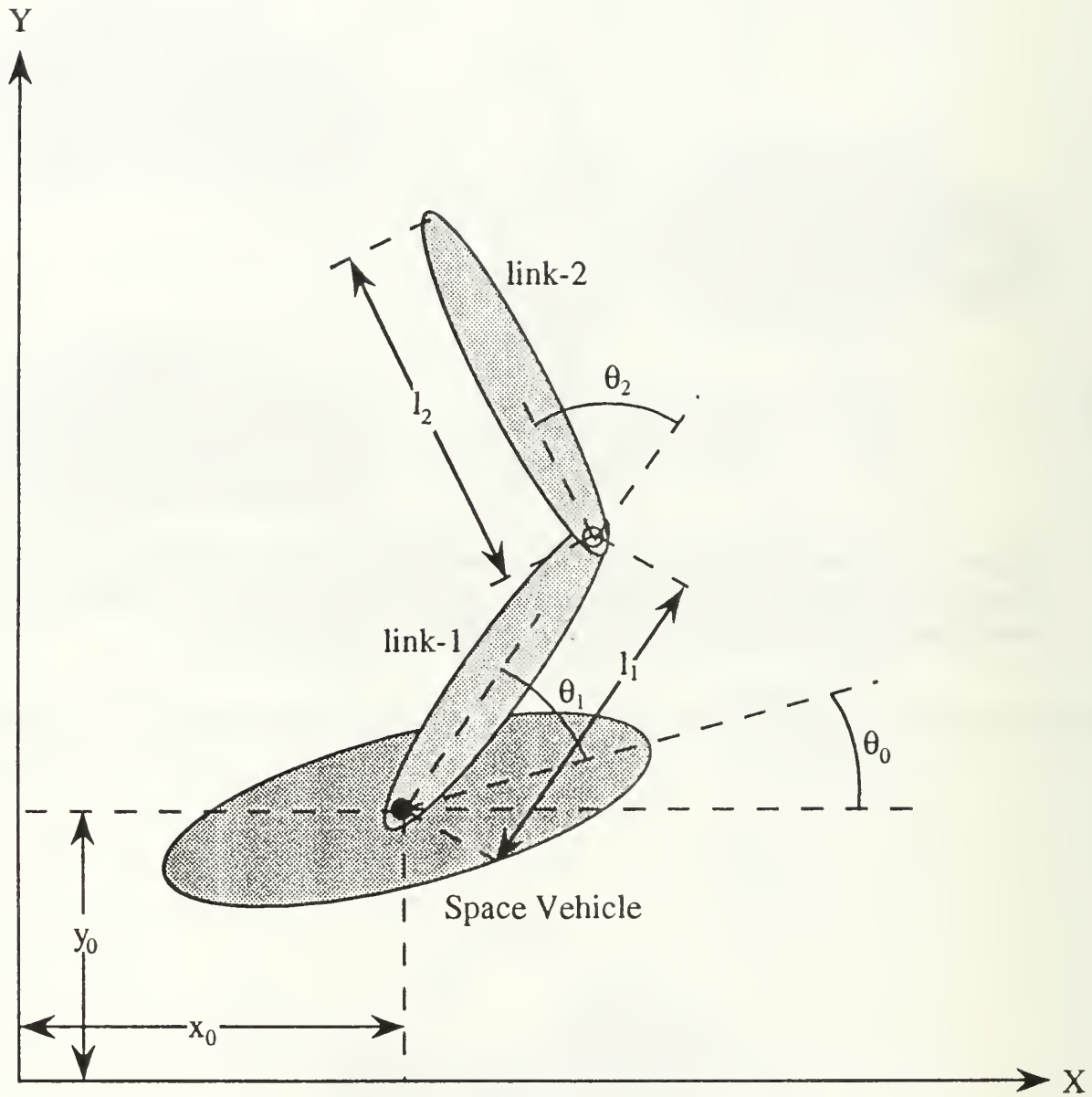

Figure 4. A two-link manipulator mounted on a space vehicle is described by three generalized coordinates: θ_0, θ_1, θ_2. The center of mass of the space vehicle has the coordinates x_0, y_0.

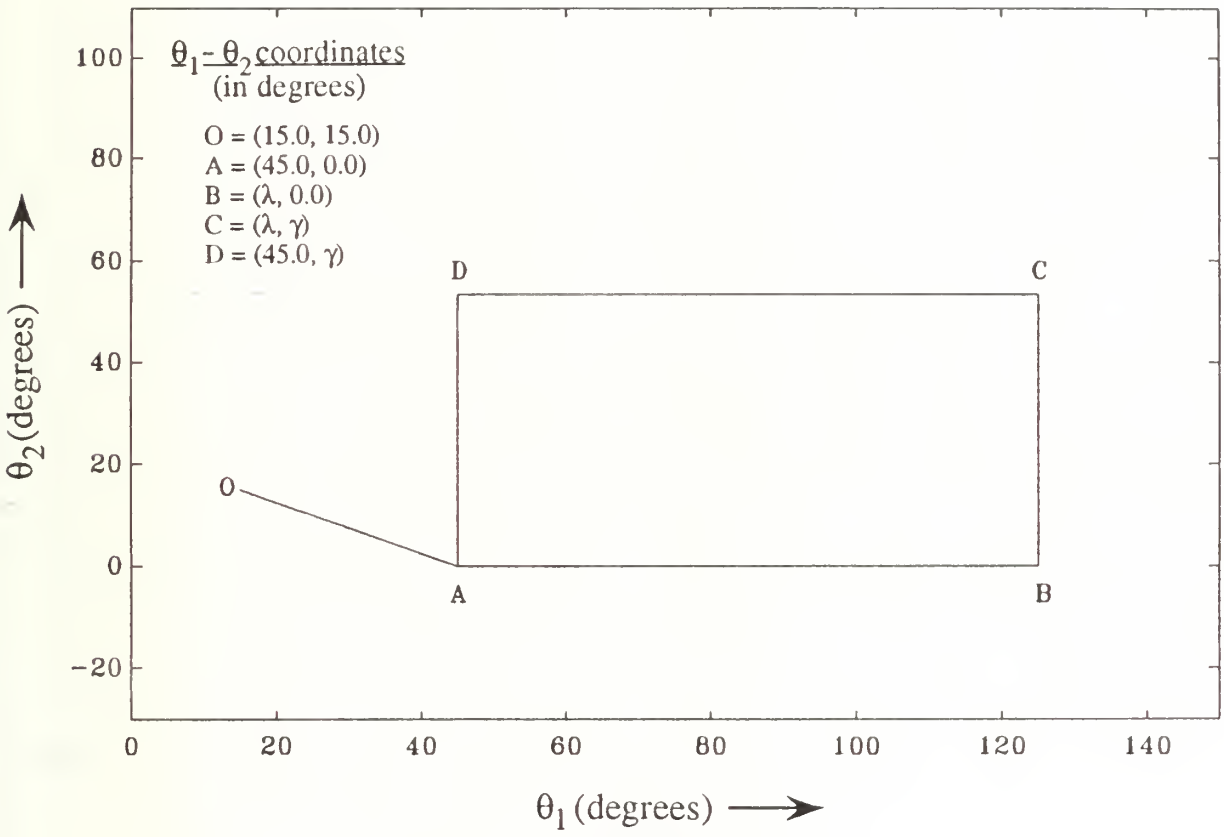

Figure 5. The path segment OA followed by the closed path ABCDA was used to converge all the configuration variables of the space robot, for the simulation discussed in section 4.1. The closed path was repeated 3 times.

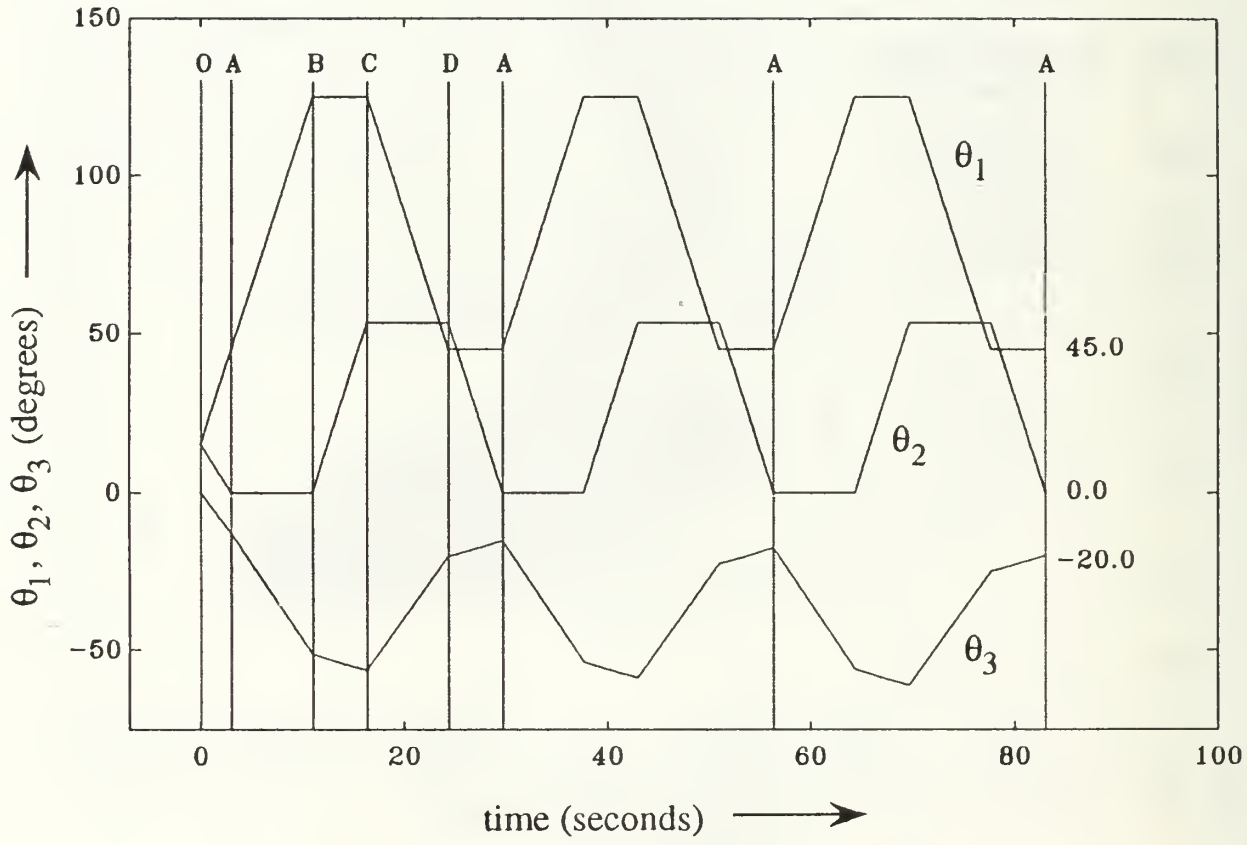

Figure 6. Evolution of all the configuration variables of the space robot with time, for the simulation discussed in section 4.1. Points O, A, B, C and D in this figure correspond to the same points in Fig.5.

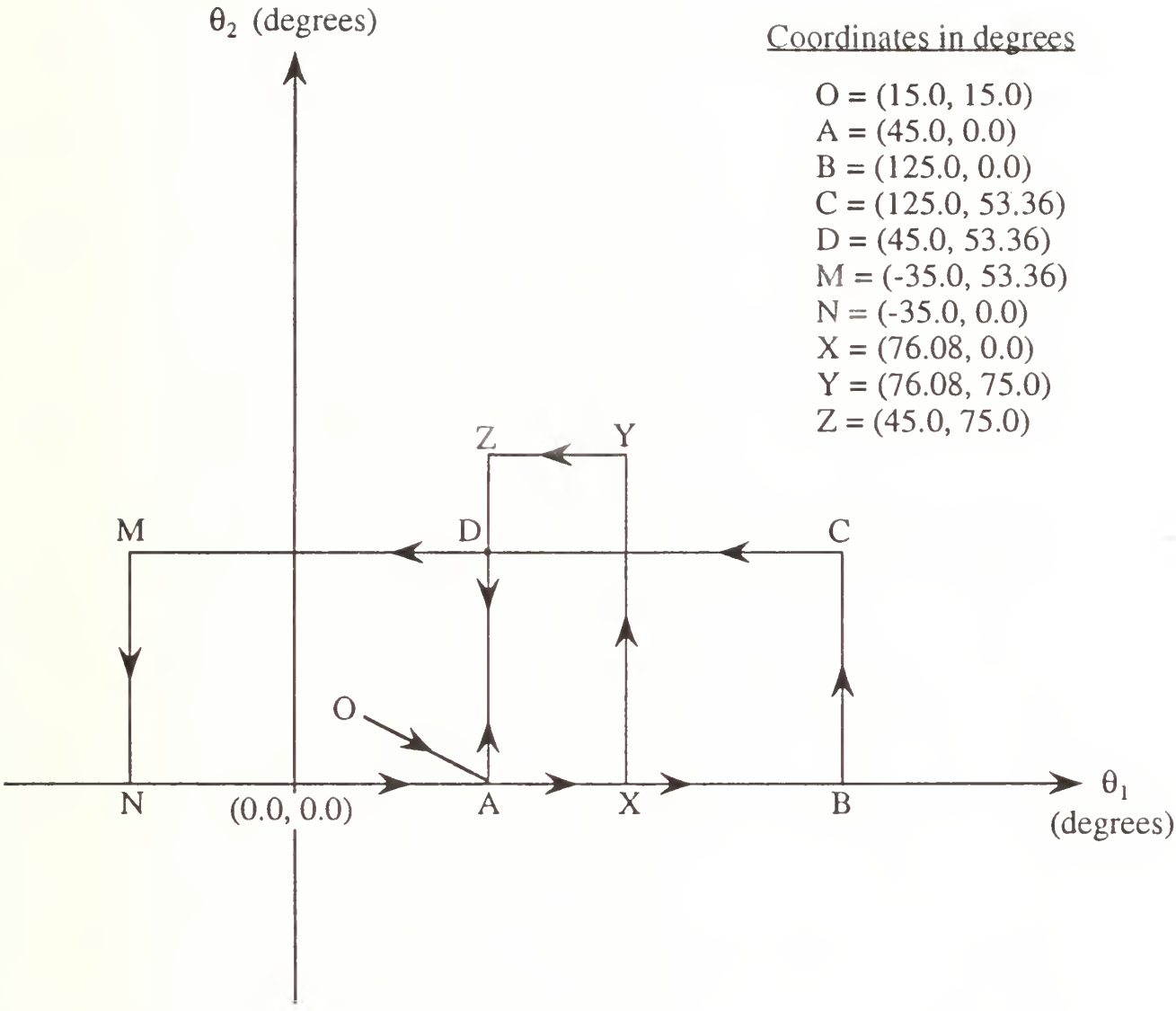

Figure 7. Directed paths ABCD, and ADMN both change the orientation of the space vehicle by equal amounts. The closed path AXYZ changes the orientation of the vehicle in four cycles by the same amount that the closed paths ABCD and ADMN can bring about in three cycles.

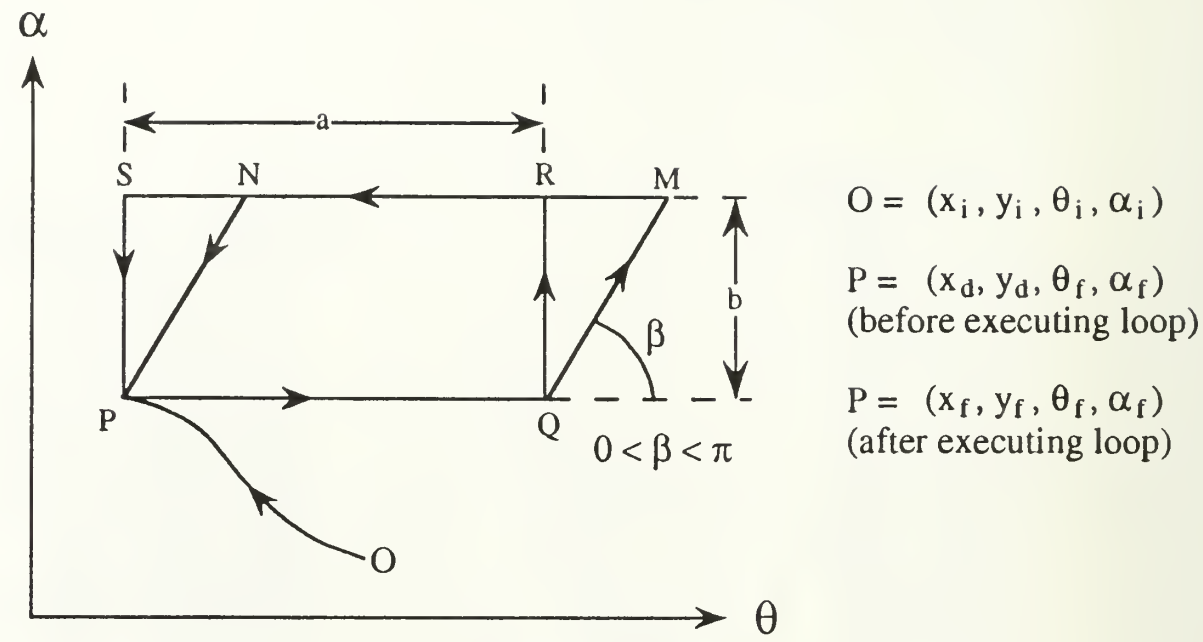

Figure 8. Both the closed paths PQRSP and PQMNP in the θ–α plane produce the same desired changes in the dependent variables x and y.

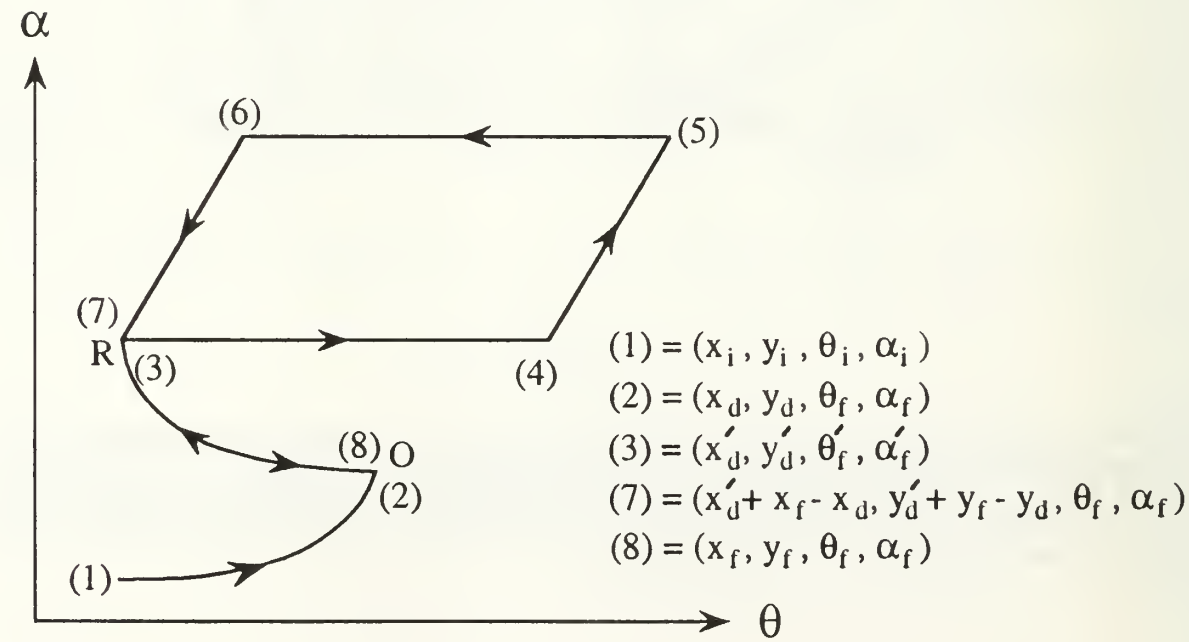

Figure 9. A diagrammatic representation of the singularity avoidance scheme

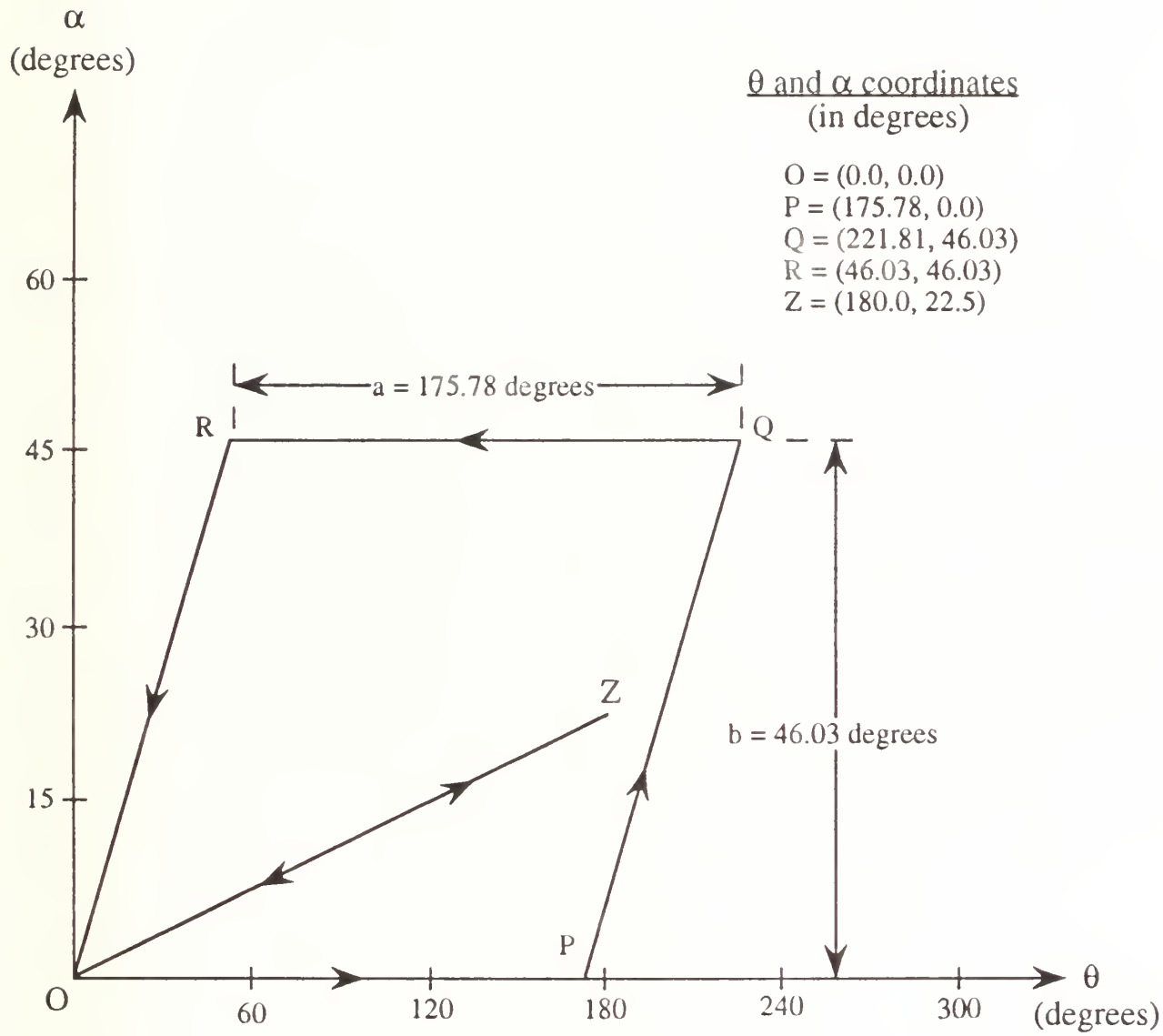

Figure 10. The path OPQROZ is the outcome of the successful implementation of the singularity avoidance scheme for the rolling disk, discussed in section 4.2.

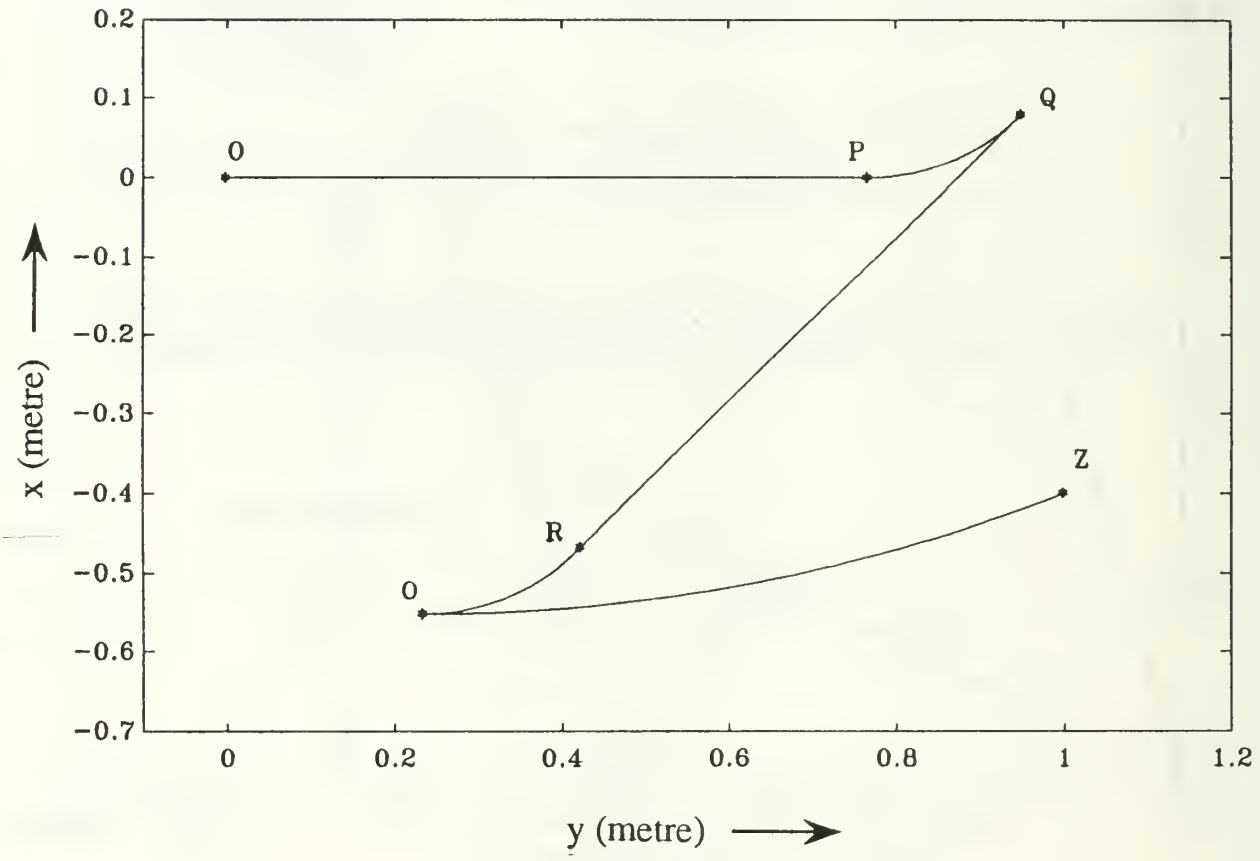

Figure 11. Path OPQROZ shows the motion of the disk rolling on the x-y plane, for the simulation discussed in section 4.2 on the singularity avoidance scheme. Fig. 10 shows the motion of the disk on the $\theta-\alpha$ plane.

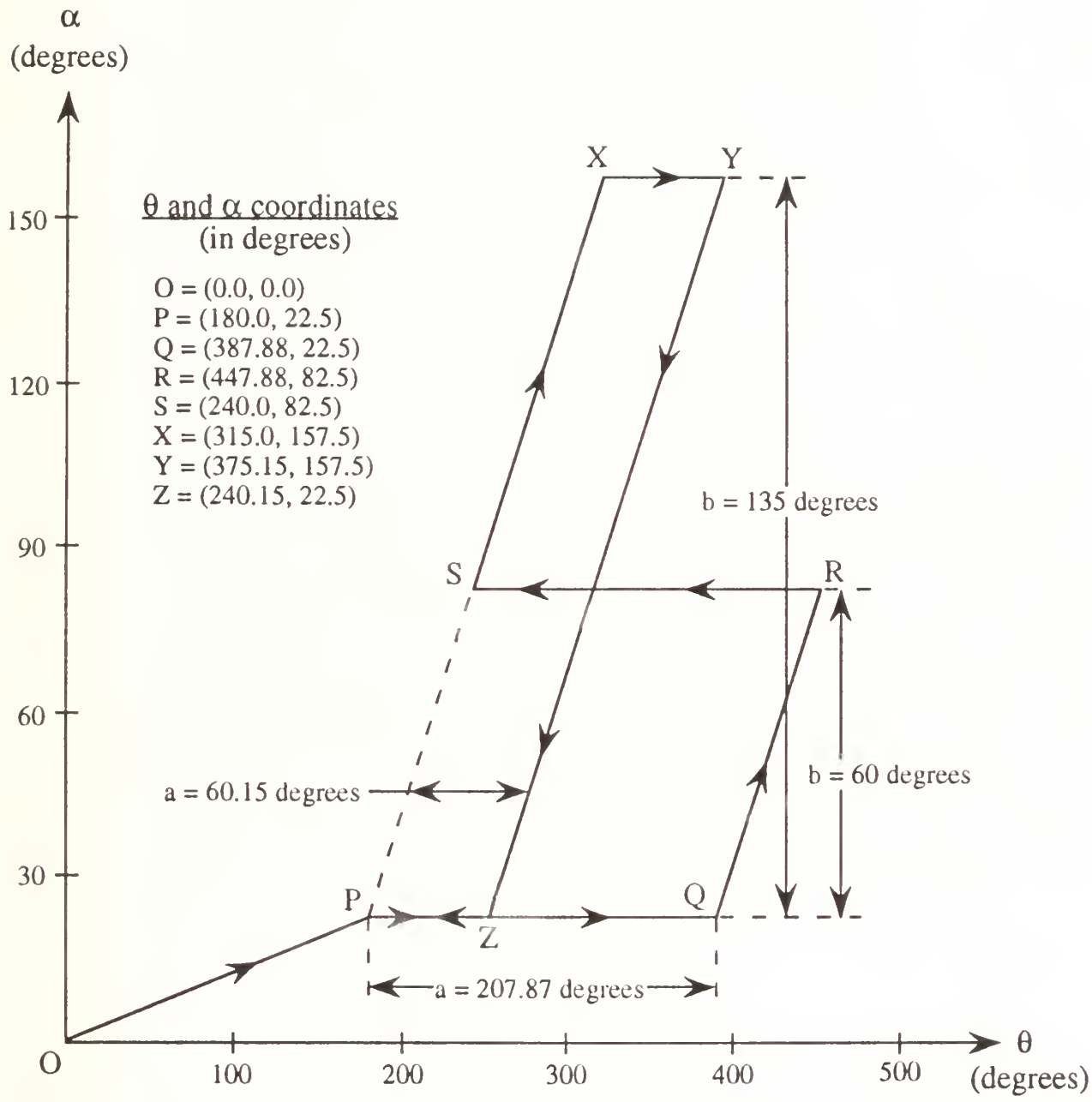

Figure 12. The path OPQRSXYZP was planned using the singularity free algorithm with a repeatable motion in the x coordinate

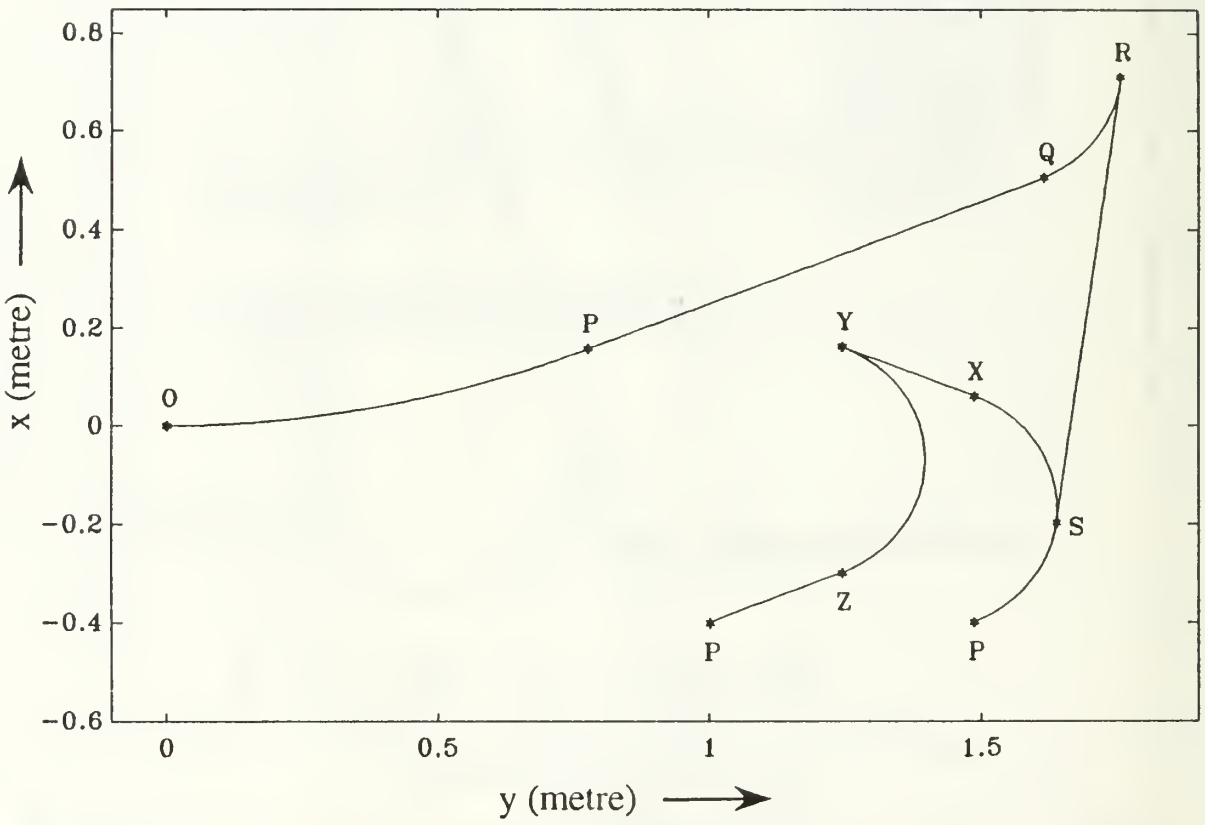

Figure 13. Path OPQRSXYZP shows the motion of the disk rolling on the x-y plane. This motion was planned using the singularity-free algorithm, discussed in section 4.2, with a repeatable motion in the x coordinate. The corresponding motion of the disk in the $\theta-\alpha$ plane is shown in Fig.11.

DISTRIBUTION LIST

1.	Defence Technical Information Center Cameron Station Alexandria, VA 22304-6145	2
2.	Library, Code 0142 Naval Postgraduate School Monterey, CA 93943-5002	2
3.	Superintendent Naval Postgraduate School Attn. Professor Ranjan Mukherjee, Code ME/Mk Monterey, CA 93943-5004	6
4.	Research Office Naval Postgraduate School Code 08 Monterey, CA 93943	1